Journal of
Applied Crystallography
ISSN 0021-8898

Octanol-rich and water-rich domains in dynamic equilibrium in the pre-ouzo region of ternary systems containing a hydrotrope

Olivier Diat, Michael L. Klossek, Didier Touraud, Bruno Deme, Isabelle Grillo, Werner Kunz and Thomas Zemb

J. Appl. Cryst. (2013). **46**, 1665–1669

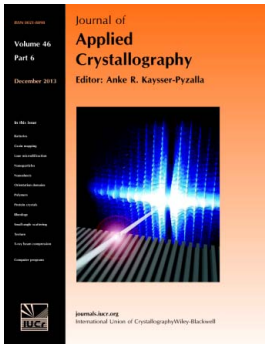

Journal of Applied Crystallography covers a wide range of crystallographic topics from the viewpoints of both techniques and theory. The journal presents papers on the application of crystallographic techniques and on the related apparatus and computer software. For many years, the *Journal of Applied Crystallography* has been the main vehicle for the publication of small-angle scattering papers and powder diffraction techniques. The journal is the primary place where crystallographic computer program information is published.

Journal of
Applied Crystallography
ISSN 0021-8898

Received 19 May 2013
Accepted 20 September 2013

Octanol-rich and water-rich domains in dynamic equilibrium in the pre-ouzo region of ternary systems containing a hydrotrope[1]

Olivier Diat,[a]* Michael L. Klossek,[b] Didier Touraud,[b] Bruno Deme,[c] Isabelle Grillo,[c] Werner Kunz[b] and Thomas Zemb[a]

[a]Institut de Chimie Séparative de Marcoule, UMR5257 CEA/CNRS/UM2/ENSCM, Bat 426, Marcoule, Bagnols sur Cèze, 30207, France, [b]Institute of Physical and Theoretical Chemistry, Universtity of Regensburg, Regensburg, 93040, Germany, and [c]Institut Laue–Langevin, 6 rue Jules Horowitz, Grenoble Cedex 9, 38042, France. Correspondence e-mail: olivier.diat@cea.fr

Ternary mixtures of medium-chain fatty alcohols, water and a hydrotrope (such as ethanol), near the immiscibility gap, make stable single phases at constant temperature. Interestingly, in this 'pre-ouzo region' these single phases consist of two distinct nanoscopic pseudo-phases, one octanol-rich and one water-rich. This domain of composition, which is known to produce strong light scattering and to separate under ultracentrifugation into two phases, has been studied using contrast variation in small-angle neutron scattering (SANS) combined with small- and wide-angle X-ray scattering (SWAXS). The existence of fatty alcohol-rich domains of well defined size of the order of 2 nm radius is proven. The scattering can be approximated by an Ornstein–Zernike function, which is close to the general expression of Choi, Chen, Sottmann & Strey [*Physica B*, (1998), **241–243**, 976–978] with vanishing quadratic Porod term. Exploitation of the relative intensities at the vanishing scattering angle in SANS demonstrates that the distribution coefficient of ethanol between the octanol-rich and the water-rich domains is close to one. WAXS of the two coexisting pseudo-phases is compared with the corresponding binary water–ethanol and octanol–ethanol samples.

1. Introduction

We consider poorly miscible, but not immiscible, liquids like water and octanol. The water–octanol miscibility gap is closed by adding a hydrotrope. The most common hydrotrope is ethanol (Zana, 1995), which is used in the cosmetics, pharmaceutics and health care industries. Ternary solutions containing alcohols have been demonstrated to show long lasting effect in olfaction (Drapeau *et al.*, 2009) and enhanced enzymatic activity (Khmelnitsky *et al.*, 1989, 1990; Zoumpanioti *et al.*, 2006). The water/ethanol/C8-alkanol phase diagrams show a critical point (Moriyoshi *et al.*, 1989). Binary ethanol–water solutions have been considered as living transient three-dimensional labile networks of hydrogen bonds. The existence of this network, with enhanced electronic density due to more oxygen atoms and fewer CH_2 groups, is the origin of the broad peak observed in wide-angle X-ray scattering (WAXS; Misawa, 2002; Takamuku *et al.*, 2004, 2005). In the ternary phase diagrams, near the critical point, the two-phase region is designated the 'ouzo' region (Vitale & Katz, 2003; Grillo, 2003; Sitnikova *et al.*, 2005). When ethanol is in excess and a single-phase region is formed, we call these compositions the 'pre-ouzo' region (Diat, 2012).

In the pre-ouzo region, dynamic as well as Rayleigh light scattering reveals the presence of large transient aggregates, similar to microemulsions so far as light scattering is considered, but without any surfactant in the formulation (Danielsson & Lindman, 1981; Chevalier & Zemb, 1990). Among the tens of thousands of papers dealing with microemulsions, less than ten refer to surfactantless micelles or microemulsions (Smith *et al.*, 1977; Keiser *et al.*, 1979). By combining small-angle neutron scattering (SANS) contrast variation and small- and wide-angle X-ray scattering (SWAXS) on a suitable q window, we investigate here the microstructure of a typical sample in the single-phase pre-ouzo region. Our aim is to determine whether the hypothesis of the presence of microemulsion or micelles based on ultracentrifugation (Borys *et al.*, 1979; Lund & Holt, 1980) can be experimentally confirmed.

2. Experimental

The procedure for the preparation of a sample is trivially simple: it only involves mixing water, a very poorly miscible fluid such as octanol and any molecule from the class of

[1] This article will form part of a virtual special issue of the journal, presenting some highlights of the 15th International Small-Angle Scattering Conference (SAS2012). This special issue will be available in late 2013/early 2014.

Table 1
Composition of sample and each of the water-rich and oil-rich parts after SANS curve analysis in volume fraction (%).

	Sample composition (±0.1%)	Water-rich domain (±0.1%)	Oil-rich domain (±0.1%)
Water	34.3	31.2	3.1
Ethanol	44.6	23.0	21.7
Octanol	21.1	3.8	17.22
Total	100	58	42

hydrotropes in the clear single-phase domain beyond but close to the miscibility gap (see supplementary material).[2]

The composition of the sample in volume fractions of the different components is given in Table 1.

In order to obtain different contrast in scattering length densities (see table in the supplementary material), the deuterated material was mixed with hydrogenated material in order to match some of the species:

For contrast P1, octanol is used in the protonated form, ethanol-D and water being fully and partially deuterated (ethD/ethH: 96/4, % volume), respectively, to achieve approximate contrast matching.

For contrast P3, protonated water is used and added to a mixture of ethanol-D and octanol, which are fully and partially deuterated (octD/octH: 89.8/10.2, % volume), respectively, to achieve approximate contrast matching.

Finally for contrast P2, the ethanol is fully protonated and diluted in D20 and partially deuterated octanol (octD/octH: 93.7/6.3, % volume) to achieve contrast matching.

The SANS measurements were performed at ILL (France) on spectrometer D33 in monochromatic mode. Standard corrections were applied: transmission normalization, empty cell and incoherent background subtraction, and absolute intensity scaling. SAXS/WAXS was performed on a Xenocs camera offering a combination of hard X-rays, a large SWAXS q window on the same detector (Mar345 image plate), and routine absolute scaling *versus* a water and polyethylene sample for normalization (Cambedouzou & Diat, 2012).

3. Results and discussion

In Fig. 1, the small-angle neutron scattering curves for a given sample (34.3% volume of water, 44.6% volume of ethanol and 21.1% volume of octanol) at three different contrasts, as mentioned in the previous paragraph, are plotted. In a first assumption, if we consider a mixture of an oil-rich domain (octanol will be considered as the oily component in these ternary systems) embedded in a water-rich phase and between which ethanol is partitioned, the P1 and P3 contrasts allow us to visualize both domains with two different scattering length densities and the P2 contrast allows us to indirectly visualize these domains by 'observing' the ethanol distribution variation between the two phases.

[2] Supplementary material discussed in this paper is available from the IUCr electronic archives (Reference: DH5008). Services for accessing this material are described at the back of the journal.

Firstly, the distribution coefficient of ethanol between polar and apolar pseudo-phases, *i.e.* between octanol-rich and water-rich phases, can be determined by generalizing the method used by Ricoul *et al.* (1997) and Demé & Zemb (2000), considering the fact that localization of solutes in aggregates influences the absolute intensities when all protonated/deuterated (H/D) combinations are used on the same sample.

The scattering by domains in microemulsions can be expressed most generally as an inverse eigth-order polynomial in q (Chen & Choi, 1997; Chen *et al.*, 1998; Choi *et al.*, 1998, 1999, 2002). This is reduced in practice to an Ornstein–Zernike (OZ)-type inverse quadratic function if the length linked to spontaneous curvature and the Porod surface term (q^{-4}) vanishes or cannot be detected:

$$I(q) = \varphi_{OR}(1-\varphi_{OR})(\rho_{OR}-\rho_{WR})^2 \frac{C\xi^3}{1+\xi^2q^2+0(q^4)} + B,$$

where φ_{OR} is the oil-rich domain volume fraction; ρ_{OR} and ρ_{WR} are the scattering densities of oil-rich and water-rich domains, respectively. The constant C is a numerical constant very close to one and related to nonspherical shape and interfacial 'smoothness' and B is a possible low incoherent background left after standard subtraction procedures.

If we consider first that the partial molar volume of each species does not vary too much [less than 6% for a water molecule in pure ethanol and less than 1% for ethanol in pure water (Moore, 1972)] and second, as mentioned previously, that ethanol is partitioned between water-rich and oil-rich phases, it should be easy to determine the optimal x fraction of ethanol in water to match simultaneously for each contrast the scattering intensities at $q = 0$, or more practically, to match the ratios between $I(0)$ for contrasts P1 and P3 and for contrasts

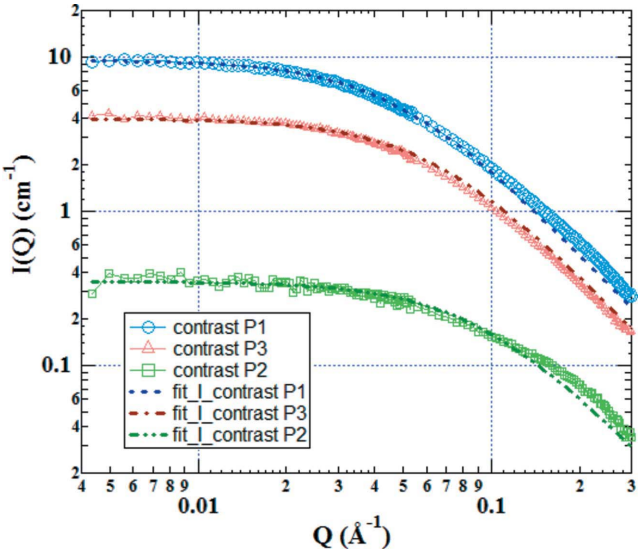

Figure 1
SANS curves produced from a sample of a solution of 44.6% volume of ethanol in water (34.3% volume) to which 21.1% volume of octanol was added at three different contrasts (P1, P2 and P3), as described in the text. The clear solution is in equilibrium with low ethanol vapour pressure in the gas phase. Best fits (dashed lines) of typical Ornstein–Zernike size ξ for the three contrasts P1, P3 and P2 are 2.1, 1.55 and 1.1 nm, respectively.

P1 and P2 (this approach allows elimination in the first step of the ξ contribution). The OZ length is determined independently from the decreasing value of q in the scattering curve and we checked *a posteriori* the right value of $I(0)$ in absolute intensity. However, we did not find any acceptable solution except if in the model adjustment we considered a fraction y of water that can be solubilized in the oil-rich phase and inversely a fraction z of octanol that can be solubilized in the water-rich part.

Thus, a minimization can be applied. A cut through the three-parameter diagram is shown in Fig. 2, where the vertical dotted line represents the optimal set of various fractions: x = 51.5% volume of ethanol in the water-rich domain, y = 9% volume of water in the oil-rich domain and z = 18% volume of oil in the water-rich part. Then, after the determination of the partitioning of the various species in each domain (see values in Table 1), the SANS curves for the different contrast can be adjusted by the OZ model in absolute scale. We found for the three contrasts different OZ sizes but of the same order of magnitude, 2.1, 1.6 and 1.1 nm for P1, P3 and P2, respectively, and a C value of five. We can consider P1 and P3 to be relatively similar, since the labelled domains are almost identical. However, it seems that this is not the case for the P2 contrast (for which only ethanol is protonated in a relatively contrast matched water/oil mixture). We found a lower value and this could be explained by a slight excess of the hydrotrope at the interface between the two phases.

Thus, from this first structural analysis, one can conclude that about 50% of the ethanol is in the water-rich domain in the pre-ouzo regime. This is consistent with the strong variation in the location of ethanol in the ouzo or two-phase domain, *i.e.* when the two coexisting phases are separated and

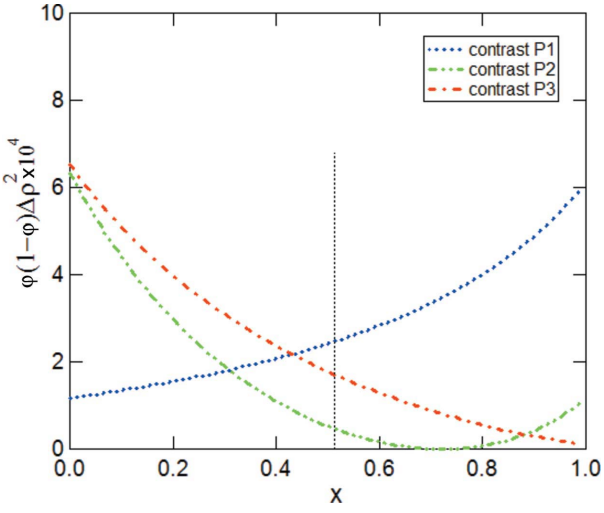

Figure 2
Plots of the scattering intensities at zero angle (cm^{-1}), as a function of the ethanol volume fraction x in water-rich domains and for a given fraction y of water in the oil-rich phase and a fraction z of oil in the water-rich phase. The optimum that allows matching of the ratios between each contrast corresponds to y and z values of 0.09 and 0.18, respectively, and an x value of 51.5% volume as indicated by the vertical dotted line. The distribution coefficient of ethanol is therefore established to be close to one between both phases.

can be analysed chemically: in the ouzo domain the ethanol partition varies with composition, and is lower than one, in the range 0.3–0.8 (Moriyoshi *et al.*, 1989). The distribution coefficient in this region has been studied at different pressure and it was shown that the ethanol distribution coefficient is about three in favour of octanol at low concentration and decreases very quickly at higher concentration to invert in favour of water in the single-phase pre-ouzo region investigated here. Translated into the log-p language used in chemical engineering, this would mean that the log-p values of ethanol vary from −0.5 at zero ethanol concentration, get close to zero in the ouzo region and reach zero in the pre-ouzo region.

Last but not least, the WAXS spectrum also allows an identification of local structures by examining high-q behaviour. Indeed, partition of added alcohol in water-rich and octanol-rich microphases produces a microemulsion-like neutron scattering pattern with typical size ξ close to 2 nm. However, in the SANS patterns, the internal structure of the two pseudo-phases present cannot be determined. Fig. 3(*a*) shows the SWAXS pattern produced by the same sample investigated by neutron scattering. First, there was no significant difference depending on the H/D labelling (see supplementary material). All scattering curves for the same sample are superimposed, except perhaps at very low q values. At larger q values, the WAXS part shows one broad peak at around q = 1.6 nm^{-1}, which seems to be composed of two contributions.

Using the volume fraction determined from SANS experiments and calculating the associated scattering length densities from the electron distribution, we can adjust the same OZ equation on the SAXS part of the scattering curve. This is shown by the dotted black curve in Fig. 3(*a*). The fitting parameters are thus C = 1 and ξ = 1.66 nm, a correlation length similar to what was obtained from neutron experiments.

Then the WAXS part can also be analysed by using the partitioning information obtained from absolute values of the scattering intensity at vanishing q values. We can indeed consider that the water-rich domain is mostly composed of water and ethanol and, inversely, the oil-rich domain is mostly composed of a mixture of octanol and ethanol.

The WAXS spectra of the sample can then be compared with those in binary systems of equivalent relative fraction as shown in Fig. 3(*b*). These relative fractions are given in Table 1 for the sample studied in this article and are close to 40/60 of ethanol/water in the water-rich part and close to 60/40 of octanol/ethanol in the oil-rich part. In a crude approach, if we apply a linear combination of 60/40 to both curves measured from the binary systems (see supplementary material), the resulting scattering curve reproduces quite well the experimental data for the ternary system, as shown in Fig. 3(*b*) (compare the dotted line with the experimental red data points).

It is important to note that the inner scattering peak in the medium-q range, which is characteristic of these alcohol systems, does not appear in the microemulsion scattering curve (Tomsic *et al.*, 2007). This peak has been the subject of a large number of simulations from molecular dynamics for

binary solvent systems (Akiyama *et al.*, 2004; Chen & Siepmann, 2006). Fewer studies have been made on a ternary mixture of the solvent. It is known from molecular dynamics that ethanol in water produces a dynamic three-dimensional bicontinuous network of strong EtOH–H_2O–EtOH hydrogen bonds. At above 5% mass of ethanol in water, this network is highly cross-linked and the surface tension towards air of the ethanol–water mixture becomes independent of ethanol content (Yano, 2005). In this pre-ouzo regime, the oil-rich domain seems to form nanometric droplets that fluctuate in a bicontinuous and water-rich medium.

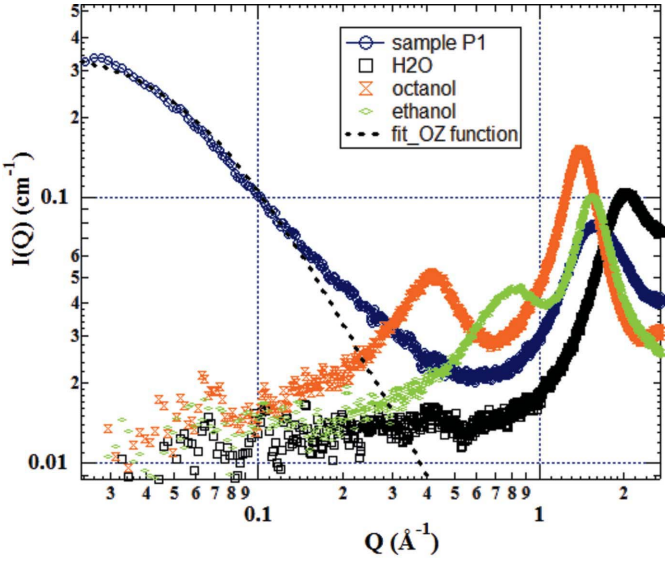

(*a*)

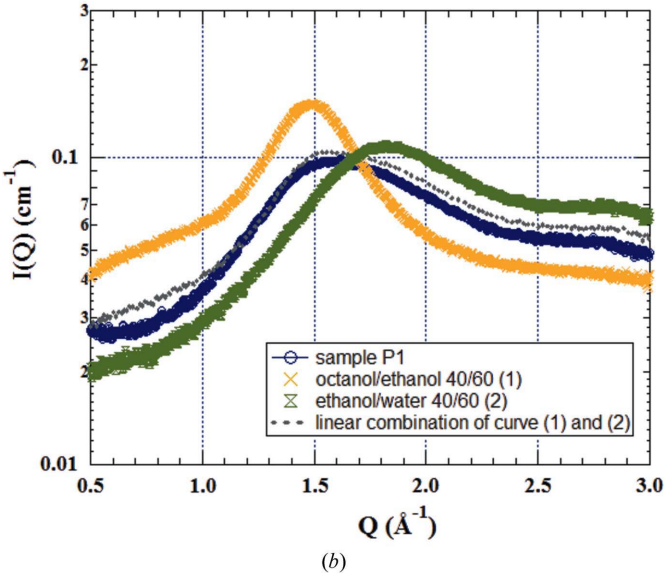

(*b*)

Figure 3
(*a*) SWAXS spectra on a log–log scale and in absolute units for the contrast P1 investigated also by SANS, compared to WAXS patterns of pure octanol, pure ethanol and water. (*b*) Magnification of the Q area between 0.5 and 2.5 Å^{-1} of (*a*) in a semi-log representation. The blue data points correspond to the WAXS signature of the contrast P1. Orange and dark-green curves correspond to the WAXS signature of binary systems of ethanol in water and 40/60 of octanol in ethanol, respectively. The black dotted curve corresponds to the linear combination of the orange and dark-green curves with a fraction of 40/60 close to the relative fractions of oil- and water-rich domains.

4. Conclusion

We can conclude, from comparison of data in Fig. 3, that the water-rich domains are structured in a very similar manner to binary ethanol–water mixtures and that the oil-rich domains are less structured than the pure corresponding liquids, since they are mainly composed of two alcohol molecules, with one hydrogen bond per molecule instead of 3.5 for water. Pure octanol, ethanol and their mixtures with dissymmetry in composition are more organized liquids in the pseudo-bulk than in the oil-rich domains investigated here, since they show a broad band in WAXS centred around 5 nm^{-1} that does not appear in the scattering signal of the pre-ouzo sample This is likely to be related to the vapour pressure paradox measured in these samples: the initial alcohol content is lowered by partial transfer of 50% of the ethanol molecules in the oil-rich domains. One would expect a decrease in activity of ethanol of the same order of magnitude, but, according to values of estimated ethanol vapour pressures (Moriyoshi *et al.*, 1989), the reduction in ethanol activity is 75%. This can only be explained by a strong adsorption of some ethanol molecules onto interfaces of water-rich or oil-rich domains. This is also why the Ornstein–Zernike length is smaller in the case of the P2 contrast. The thermodynamics of this interface in detergentless microemulsions, and their structure and surface pressures, are currently under investigation and will be the subject of a forthcoming paper.

As far as applications are concerned, ternary solutions in the pre-ouzo region are excellent solubilizers in terms of formulation (Zoumpanioti *et al.*, 2006; Bauduin *et al.*, 2008; Drapeau *et al.*, 2009), since the ethanol is a co-solute of the fatty alcohol. We are aware that this general principle of opposing forces fixing the size of the formed micelles allows 'green' detergentless formulation of so-called 'hydroalcoholic' solutions and will open new routes for formulation of innovative 'low-alcohol' microemulsions or solubilization with alternative hydrotropes.

References

Akiyama, I., Ogawa, M., Takase, K., Takamuku, T., Yamaguchi, T. & Ohtori, N. (2004). *J. Solution Chem.* **33**, 797–809.
Bauduin, P., Testard, F. & Zemb, T. (2008). *J. Phys. Chem. B*, **112**, 12354–12360.
Borys, N. F., Holt, S. L. & Barden, R. E. (1979). *J. Colloid Interface Sci.* **71**, 526–532.
Cambedouzou, J. & Diat, O. (2012). *J. Appl. Cryst.* **45**, 662–673.
Chen, B. & Siepmann, J. I. (2006). *J. Phys. Chem. B*, **110**, 3555–3563.
Chen, S.-H. & Choi, S.-M. (1997). *J. Appl. Cryst.* **30**, 755–760.
Chen, S.-H., Choi, S.-M. & LoNostro, P. (1998). *Nuovo Cimento Soc. Ital. Fis. D*, **20**, 1971–1988.
Chevalier, Y. & Zemb, T. (1990). *Rep. Prog. Phys.* **53**, 279.
Choi, S.-M., Chen, S.-H., Sottmann, T. & Strey, R. (1998). *Physica B*, **241–243**, 976–978.
Choi, S. M., Chen, S. H., Sottmann, T. & Strey, R. (2002). *Physica A*, **304**, 85–92.

Choi, S.-M., LoNostro, P. & Chen, S.-H. (1999). *Trends in Colloid and Interface Science XIII*, *Progress in Colloid and Polymer Science*, Vol. 112, edited by Durdica Tezak & Mladen Martinis, pp. 98–104. Berlin, Heidelberg: Springer.
Danielsson, I. & Lindman, B. (1981). *Colloid. Surf.* **3**, 391–392.
Demé, B. & Zemb, T. (2000). *J. Appl. Cryst.* **33**, 569–573.
Diat, O. (2012). *Proceedings of the 15th International Small-Angle Scattering Conference, Sydney, Australia, 18–23 November 2012*, edited by Duncan J. McGillivray, Jill Trewhella, Elliot P. Gilbert & Tracey L. Hanley. Lucas Heights: ANSTO.
Drapeau, J., Verdier, M., Touraud, D., Kröckel, U., Geier, M., Rose, A. & Kunz, W. (2009). *Chem. Biodiver.* **6**, 934–947.
Grillo, I. (2003). *Colloid. Surf. A Physicochem. Eng. Aspects*, **225**, 153–160.
Keiser, B. A., Varie, D., Barden, R. E. & Holt, S. L. (1979). *J. Phys. Chem.* **83**, 1276–1280.
Khmelnitsky, Y. L., Gladilin, A. K., Neverova, I. N., Levashov, A. V. & Martinek, K. (1990). *Collect. Czech. Chem. Commun.* **55**, 555–563.
Khmelnitsky, Y. L., Van Hoek, A., Veeger, C. & Visser, A. J. W. G. (1989). *J. Phys. Chem.* **93**, 872–878.
Lund, G. & Holt, S. L. (1980). *J. Am. Oil Chem. Soc.* **57**, 264–267.
Misawa, M. (2002). *J. Chem. Phys.* **116**, 8463–8468.
Moore, W. J. (1972). *Physical Chemistry*, 4th ed. New Jersey: Prentice-Hall.
Moriyoshi, T., Sakamoto, T. & Uosaki, Y. (1989). *J. Chem. Thermodyn.* **21**, 947–954.
Ricoul, F., Dubois, M. & Zemb, T. (1997). *J. Phys. II Fr.* **7**, 69–77.
Sitnikova, N. L., Sprik, R., Wegdam, G. & Eiser, E. (2005). *Langmuir*, **21**, 7083–7089.
Smith, G. D., Donelan, C. E. & Barden, R. E. (1977). *J. Colloid Interface Sci.* **60**, 488–496.
Takamuku, T., Maruyama, H., Watanabe, K. & Yamaguchi, T. (2004). *J. Solution Chem.* **33**, 641–660.
Takamuku, T., Saisho, K., Nozawa, S. & Yamaguchi, T. (2005). *J. Mol. Liq.* **119**, 133–146.
Tomsic, M., Jamnik, A., Fritz-Popovski, G., Glatter, O. & Vlcek, L. (2007). *J. Phys. Chem. B*, **111**, 1738–1751.
Vitale, S. A. & Katz, J. L. (2003). *Langmuir*, **19**, 4105–4110.
Yano, Y. F. (2005). *J. Colloid Interface Sci.* **284**, 255–259.
Zana, R. (1995). *Adv. Colloid. Interface Sci.* **57**, 1–64.
Zoumpanioti, M., Karali, M., Xenakis, A. & Stamatis, H. (2006). *Enzyme Microbiol. Technol.* **39**, 531–539.